JOURNAL OF GEOPHYSICAL RESEARCH: EARTH SURFACE, VOL. 118, 2045–2058, doi:10.1002/jgrf.20143, 2013

Inferring tidal wetland stability from channel sediment fluxes: Observations and a conceptual model

Neil K. Ganju,[1] Nicholas J. Nidzieko,[2] and Matthew L. Kirwan[3]

Received 14 February 2013; revised 29 August 2013; accepted 4 September 2013; published 7 October 2013.

[1] Anthropogenic and climatic forces have modified the geomorphology of tidal wetlands over a range of timescales. Changes in land use, sediment supply, river flow, storminess, and sea level alter the layout of tidal channels, intertidal flats, and marsh plains; these elements define wetland complexes. Diagnostically, measurements of net sediment fluxes through tidal channels are high-temporal resolution, spatially integrated quantities that indicate (1) whether a complex is stable over seasonal timescales and (2) what mechanisms are leading to that state. We estimated sediment fluxes through tidal channels draining wetland complexes on the Blackwater and Transquaking Rivers, Maryland, USA. While the Blackwater complex has experienced decades of degradation and been largely converted to open water, the Transquaking complex has persisted as an expansive, vegetated marsh. The measured net export at the Blackwater complex (1.0 kg/s or 0.56 kg/m^2/yr over the landward marsh area) was caused by northwesterly winds, which exported water and sediment on the subtidal timescale; tidally forced net fluxes were weak and precluded landward transport of suspended sediment from potential seaward sources. Though wind forcing also exported sediment at the Transquaking complex, strong tidal forcing and proximity to a turbidity maximum led to an import of sediment (0.031 kg/s or 0.70 kg/m^2/yr). This resulted in a spatially averaged accretion of 3.9 mm/yr, equaling the regional relative sea level rise. Our results suggest that in areas where seaward sediment supply is dominant, seaward wetlands may be more capable of withstanding sea level rise over the short term than landward wetlands. We propose a conceptual model to determine a complex's tendency toward stability or instability based on sediment source, wetland channel location, and transport mechanisms. Wetlands with a reliable portfolio of sources and transport mechanisms appear better suited to offset natural and anthropogenic loss.

Citation: Ganju, N. K., N. J. Nidzieko, and M. L. Kirwan (2013), Inferring tidal wetland stability from channel sediment fluxes: Observations and a conceptual model, *J. Geophys. Res. Earth Surf.*, *118*, 2045–2058, doi:10.1002/jgrf.20143.

1. Introduction

[2] Tidal wetland complexes are geomorphic features composed of vegetated marsh plain, intertidal flats, and tidal channels. The stability of a tidal wetland complex is a function of interconnected biogeomorphic and physical processes [e.g., *D'Alpaos et al.*, 2012]. Processes conducive to stability include root expansion [*Redfield*, 1972], biostabilization by mollusks [*Bertness*, 1984], vertical accretion through autochthonous organic deposition [*Stevenson et al.*, 1985], and accretion through allochthonous inorganic sediment deposition during inundation [*Reed et al.*, 1999]. Processes contributing to instability include subsidence [*Cahoon et al.*, 1999], vertebrate herbivory [*Ford and Grace*, 1998], saltwater intrusion and flooding [*DeLaune and Pezeshki*, 1994], bank erosion during wave attack [*van der Wal and Pye*, 2004], and eutrophication [*Deegan et al.*, 2012]. These processes are linked through positive and negative feedback loops [*Fagherazzi et al.*, 2012; *Day et al.*, 2011; *Kirwan et al.*, 2008], which complicate interpretation of wetland stability via infrequent point measurements on the marsh plain. Under present conditions of accelerating sea level rise [*Sallenger et al.*, 2012], biogeomorphic processes must respond to maintain elevation relative to sea level or else the marsh will submerge. Recent work suggests that tidal ecosystems have at least two stable equilibriums, where one is characterized by high elevations covered with productive vegetation (i.e., marsh) and the other is characterized by wave-influenced elevations too low for vegetation to persist (i.e., mudflat) [*Fagherazzi et al.*, 2006; *Marani et al.*, 2007; *Kirwan and Murray*, 2007; *D'Alpaos et al.*, 2012].

[1]U.S. Geological Survey, Woods Hole Coastal and Marine Science Center, Woods Hole, Massachusetts, USA.
[2]Horn Point Laboratory, University of Maryland Center for Environmental Science, University of Maryland, Cambridge, Maryland, USA.
[3]Virginia Institute of Marine Science, College of William Mary, Gloucester Point, Virginia, USA.

Corresponding author: N. K. Ganju, Woods Hole Coastal and Marine Science Center, 384 Woods Hole Rd., Woods Hole, MA 02556, USA. (nganju@usgs.gov)

2169-9003/13/10.1002/jgrf.20143

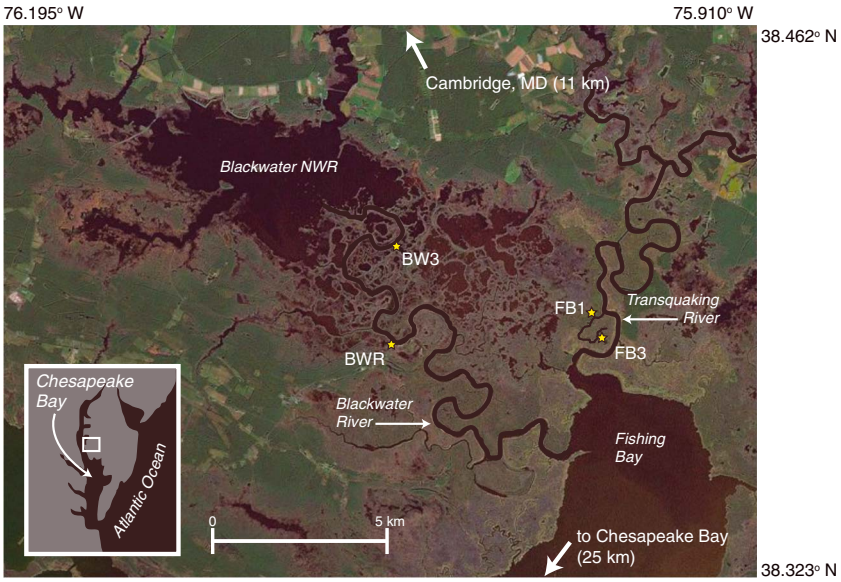

Figure 1. Site map of study area on the eastern shore of Maryland, USA. Site CAMM2 is 2 km northwest of Cambridge, MD.

Changes in physical parameters such as the rate of sea level rise and mineral sediment supply may cause a shift from one ecosystem state to the other. Here we define a stable marsh as one where a vegetated marsh will survive small perturbations to physical parameters (i.e., elevations are within the basin of attraction for an intertidal marsh) [*Scheffer et al*., 2001]. Thus, we consider a marsh to be stable if it is trending toward a vegetated equilibrium configuration, even though that may include a marsh that is far away from its equilibrium configuration.

[3] Tidal channels deliver sediment to the vegetated subaerial marsh plain on high tides, which tends to increase the elevation of the marsh plain through time [*Redfield*, 1972; *Reed et al*., 1999; see *Friedrichs and Perry*, 2001, for a comprehensive review]. However, properties of the marsh plain also influence sediment transport through the channel network by influencing flow direction, tidal prism volumes, and cross-sectional area [*D'Alpaos et al*., 2007; *Kirwan and Murray*, 2007; *Temmerman et al*., 2007; *Hood*, 2010; *Temmerman et al*., 2012]. Moreover, only a small fraction of the suspended sediment flux in a tidal channel may be directed to the marsh plain during the highest tides, and the marsh plain may contribute sediment to tidal channels through creek bank slump and other erosive processes [e.g., *Gabet*, 1998]. Prior work suggests that marsh plains and channel networks develop simultaneously, moving toward an equilibrium condition where the net sediment flux through the channel network channels equals zero, and the transfer of sediment from channel to marsh platform balances sea level rise [*Friedrichs and Perry*, 2001; *Fagherazzi et al*., 2012]. Therefore, measurements of the concentration and flux of sediments through tidal channels potentially represent a spatially integrated measure of marsh stability.

[4] Point measurements such as surface elevation [*Webb et al*., 2013], accretion [*Cahoon and Turner*, 1989], and vegetative biomass [*Kirwan and Guntenspergen*, 2012] can only resolve a limited number of locations on the wetland plain itself. For example, *Deegan et al*. [2012] highlighted the instability and rapid collapse of creek banks under nutrient-rich conditions; point observations of aboveground biomass on the marsh plain only may have inferred stability in that case. Wetland vulnerability assessments based on point measurements would suggest increasing stability with increased sediment supply and accretion; however, *Kirwan et al*. [2008] showed that some wetlands worldwide are degrading despite accretion rates that appear to offset sea level rise. Sediment flux measurements in a wetland tidal channel constrain the sediment budget of the complex and spatiotemporally integrate the effects of different mechanisms. It is therefore possible to gauge the stability of an entire complex with sediment flux measurements. Few studies have considered assessing stability via the actual mechanisms and magnitudes of sediment transport, but it is clear this will be an improvement over point measurements.

[5] In this paper we compare sediment flux measurements through tidal channels from a rapidly degrading wetland complex and a relatively stable complex, in adjacent tributaries of the Chesapeake Bay (Maryland, USA). Given the proximity yet disparate fate of the two wetland complexes, this study attempts to estimate sediment fluxes to/from each complex, identify mechanisms responsible for landward and seaward transport, and assess their stability in response to sea level rise. Finally, a conceptual framework for assessing the stability of tidal wetlands based on channel sediment fluxes is proposed.

2. Site Description

[6] The Blackwater National Wildlife Refuge (NWR) encompasses 110 km^2 on the mid-Atlantic coast of the United States and is primarily drained by the Blackwater River, which empties into Fishing Bay and ultimately Chesapeake Bay (Figure 1). The adjacent Fishing Bay Wildlife Management Area covers 120 km^2; a portion of the area is centered on the Transquaking River which also drains into Fishing Bay. Freshwater inflow to Blackwater NWR is primarily

from the Little Blackwater River and peaks at 6.0 m^3/s during winter months (http://waterdata.usgs.gov/nwis). Inflow to the Transquaking River (via the Chicamicomico River) peaked at less than 1.0 m^3/s during the period of this study. Neither tributary is considered to be a large source of sediment [*Stevenson et al*., 1985]; periodic water sampling at the Little Blackwater River during this study yielded suspended sediment concentrations (SSC) less than 10 mg/L. Spring tide range in Fishing Bay is over 1.0 m and attenuates to less than 0.20 m within the open-water area of Blackwater NWR; event-scale changes in water level caused by barometric pressure fluctuations and wind setup may exceed 1.0 m [*Wang and Elliott*, 1978].

[7] Since the early twentieth century, wetlands within Blackwater NWR have experienced extensive loss (56 ha/yr from 1938 to 1979; *Stevenson et al*., 1985]. *Stevenson et al*. [1985] suggested that sea level rise, invasive rodents, and open-water expansion led to this loss though the current rate may have slowed. Over the same period, wetlands along the adjacent Transquaking River have appeared to maintain stability and forestall open-water expansion despite their proximity to Blackwater NWR. *Stevenson et al*. [1985] attempted to quantify the net sediment export from the Blackwater River using periodic sampling for suspended sediment concentration and water flux. Their estimate of 720,000 t/yr (or 14 kg/m^2/yr) is largely based on an extrapolated estimate of the difference between ebb and flood transports over 14 tidal cycles and is likely biased by aliasing with atypical tidal conditions. If this estimate was correct, in the 30 years since their measurement, over 4.0 m of vertical elevation loss would have occurred on average over the refuge.

[8] We occupied two sites in each complex between 20 September 2011 and 9 December 2011; seaward sites (BWR, FB1) were equipped to measure sediment fluxes while landward sites (BW3, FB3) were reference stations for suspended sediment concentrations only (Figure 1). Sites FB1, BW3, and FB3 were occupied in the spring of 2011 as well (SSC data only), and those data are reported by *Ganju et al*. [2012]. Within the Blackwater River, site BWR was located in the channel seaward of the Maple Dam Road bridge at Shorter's Wharf; site BW3 was located within a channelized portion of the marsh off the Blackwater River 6.0 km landward of site BWR. In the Transquaking River we occupied two sites in a tidal creek off the main channel: FB1 was located 250 m landward of the Transquaking River confluence, while FB3 was 2.0 km farther landward.

3. Methods

3.1. Continuous Tidal Water Fluxes

[9] We can construct a continuous record of water fluxes through tidally affected channels from a continuous index velocity (v_i) and water level (h) measurement, and a less frequent record of cross-sectionally averaged velocity (v_{ca}) and channel area (a) over some representative period [*Ruhl and Simpson*, 2005]. A complete record of v_{ca} is computed using the correlation between v_i and v_{ca}, and a complete record of a is computed using h and the channel geometry. The product of v_{ca} and a from the complete record yields a continuous record of tidal water fluxes (Q_i). At sites BWR and FB1 we deployed a Nortek Aquadopp acoustic Doppler current profiler (ADCP) at approximately 0.10 m above bottom (mab) to measure v_i and h. The instrument platform was located in the center of the respective channels. Both instruments sampled over a 5 min period at 15 min intervals in 0.50 m vertical bins. Measurements of v_{ca} and a were collected with a RD Instruments 1200 kHz Rio Grande ADCP in downward looking configuration [*Mueller and Wagner*, 2009]. The surveys were performed during spring tides when the largest range of conditions was expected.

[10] During the week of 4 October 2011, we collected 226 ADCP transects just seaward of the continuously deployed ADCP. We again measured channel area (a) and geometry at high tide and cross-sectionally averaged velocity (v_{ca}) over varying flood and ebb periods on multiple days. Continuous water level measurements were obtained at all sites. The index velocity calibration at site BWR was developed using the mean velocity of the four lower bins of the Aquadopp as the index velocity v_i and the cross-sectional ADCP measurements for v_{ca} (Figure 2a). The bottom four bins cover the entire water column at low tide, so the index velocity is effectively a vertically averaged mean below the low-water line. At site FB1 the index velocity calibration was developed using the mean velocity of the three lower bins of the Aquadopp as the index velocity v_i and the cross-sectional measurements for v_{ca} (Figure 2a). Channel cross sections were measured with the ADCP at both sites during slack high water. Relationships between water level and cross-sectional area were determined with the AreaComp program, provided by the U.S. Geological Survey Office of Surface Water's Hydroacoustics Workgroup (http://hydroacoustics.usgs.gov). The tidal water flux time series at both sites were calculated as the product of v_{ca} and a.

3.2. Continuous Cross-Sectionally Averaged SSC

[11] A continuous record of cross-sectionally averaged SSC can be generated using turbidity as a proxy and relating a continuously measured point (index) value with a less frequent measurement of cross-sectionally averaged turbidity. Continuous index turbidity (NTU_i) measurements were collected at sites BWR and FB1 using YSI 6600 sondes with optical turbidity probes and at sites BW3 and FB3 with WetLabs ECO-BBSB sensors. All turbidity sensors had wipers to prevent fouling and were mounted 0.35 mab on aluminum poles driven into the channel bed adjacent to the marsh. During the same period as the ADCP surveys, a YSI 6600 sonde was deployed in profiling mode to measure vertical profiles of turbidity at five lateral locations across each channel (by bridge at site BWR and by canoe/tagline at site FB3). These measurements were interpolated to a uniform grid across the channel to estimate a cross-sectionally averaged turbidity (NTU_{ca}). Water samples were collected with a van Dorn sampler at all sites (including vertical profiling locations) to calibrate nephelometric turbidity unit (NTU) readings to suspended sediment concentrations. We also estimated the velocity-weighted cross-sectionally averaged turbidity [e.g., *Ganju and Schoellhamer*, 2006] by computing the spatially varying point flux as the product of the velocity and turbidity from the ADCP surveys and vertical turbidity profiling, respectively.

[12] Continuous time series of index turbidity were generated at sites BWR and FB1, while point turbidities were also measured at sites BW3 and FB3 for comparison. Data from

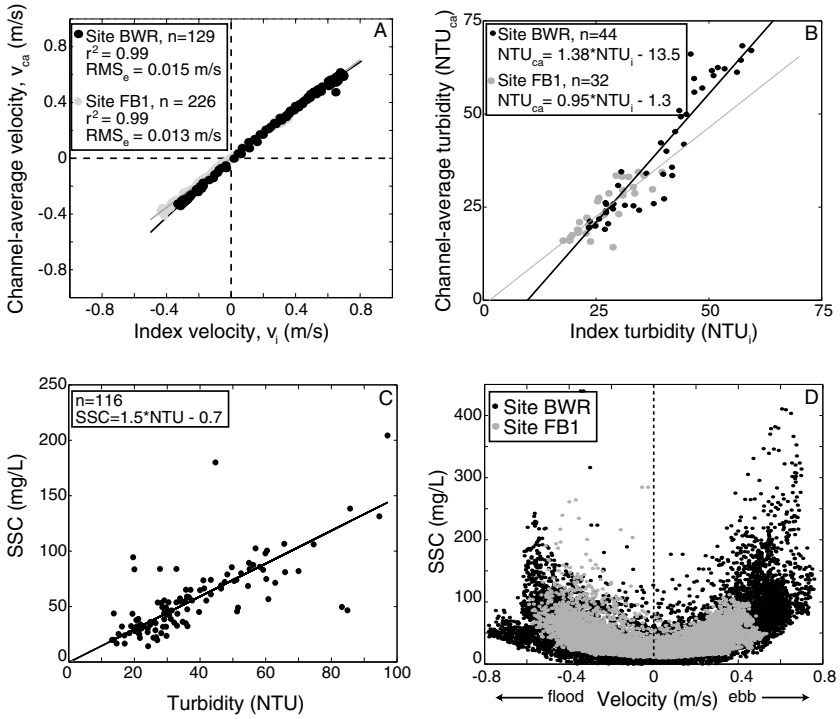

Figure 2. (a) Index velocity calibrations for sites BWR and FB1; (b) index turbidity calibrations for sites BWR (prediction interval +4 to −7 NTU; 95% CI on slope 1.29 to 1.57) and FB1 (prediction interval +4 to −2 NTU; 95% CI on slope 0.77 to 1.18); (c) turbidity-to-SSC calibration for all sites over spring and fall 2011 (prediction interval +10 to −15 mg/L; 95% CI on slope 1.24 to 1.58); and (d) velocity versus SSC for sites BWR and FB1. SSC at BWR is increased on ebb tides relative to flood tides; SSC at FB1 is increased on flood tides relative to ebb tides.

sites BW3 and FB3 were presented by *Ganju et al*. [2012] and are only discussed briefly later in the paper. Cross-sectionally averaged turbidity was estimated with 44 sets of five vertical casts at site BWR and 32 sets of five vertical casts at site FB1 during the same period as the ADCP transects. Index turbidities from sites BWR and FB1 at the midpoint time of the transects were used to generate a calibration curve to estimate continuous cross-sectionally averaged turbidity (Figure 2b). Linear calibration of NTU to SSC was performed by aggregating 116 samples collected from all sites (Figure 2c); the calibrations for individual sites using the repeated median method [*Helsel and Hirsch*, 1992] were statistically indistinguishable from each other so a combined repeated median linear calibration was used. This calibration was then applied to all turbidity time series from all sites.

3.3. Sediment Flux Decomposition

[13] Decomposing sediment fluxes provides a framework for evaluating the influence of different processes on estuarine sediment transport. Flux decomposition can typically separate the contributions from riverine input, wind-induced circulation, spatial gradients in SSC, and tidal hydrodynamic processes [e.g., *Geyer et al*., 2001; *Ganju et al*., 2005; *Ganju and Schoellhamer*, 2006]. Low-frequency forcing such as river flow and meteorological events are manifested in the advective flux while tidal cycle correlations between velocity and concentration arise as a dispersive flux. Stokes drift flux is caused by a correlation between velocity and channel area; this flux is large in systems with a progressive tidal wave.

[14] Continuous measurements of cross-sectionally averaged velocity (u), channel area (a), and cross-sectionally averaged SSC (c) are combined to yield the sediment flux as

$$F = u \times a \times c \tag{1}$$

where

$$u = u' + < u > \tag{2}$$

$$a = a' + < a > \tag{3}$$

$$c = c' + < c > \tag{4}$$

[15] Brackets indicate the tidally averaged value of the variable (via application of a 30 h low-pass filter to remove all tidal signals) while the prime denotes the remaining fluctuating part of the variable. Substituting equations (2)–(4) into equation (1) and expanding yields

$$\begin{aligned} F = &< u >< a >< c > + u' < a > c' + u'a' < c > + u'a'c' \\ &+ < u >< a > c' + < u > a'c' + u' < a >< c > \\ &+ < u > a' < c > \end{aligned} \tag{5}$$

where $<u><a><c>$ is the advective flux, $u'<a>c'$ is the dispersive flux, $u'a'<c>$ is the Stokes drift flux, and $u'a'c'$ is the triple correlation between Stokes drift flux and concentration. In most estuarine systems, the first three terms dominate and the remaining terms are negligible. Total sediment flux and individual flux components were calculated at sites BWR and FB1 following equations (1)–(5).

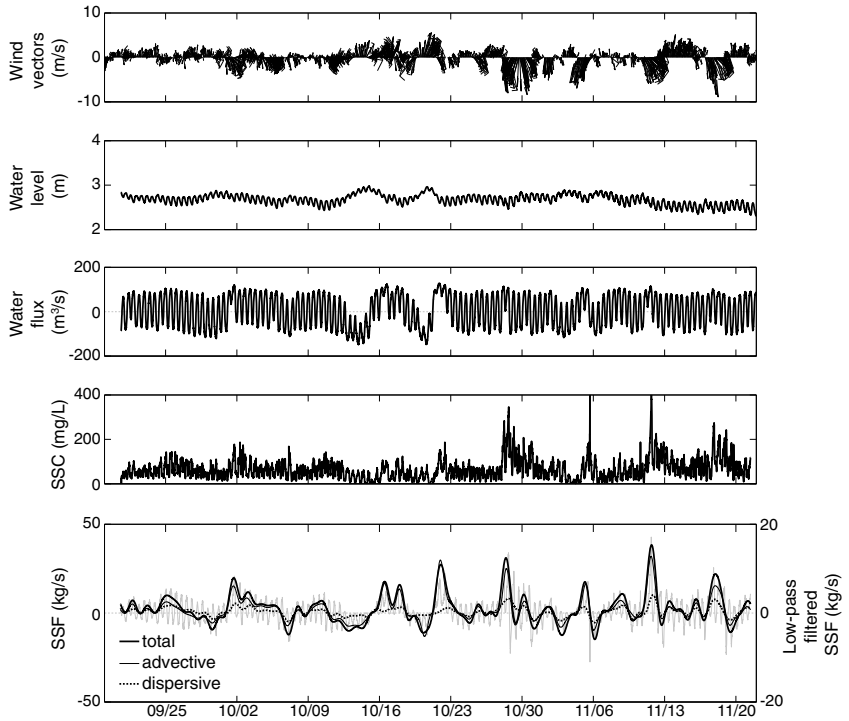

Figure 3. Time series of wind speed/direction, water level, tidal water flux, suspended sediment concentration (SSC), and suspended sediment flux (SSF) components at site BWR. Gray trace of SSF is tidal SSF; other terms are low-pass filtered. Positive water and sediment flux values indicate seaward transport. Wind vectors point in the direction the wind is going.

[16] The decomposition presented here ignores spatial correlation terms, which may be large in deep channels with stratification or channel-shoal systems. We assessed spatial correlation between velocity and turbidity by interpolating turbidity data to the same three-dimensional plane (time, depth, lateral distance) as the velocity data and then weighting turbidity values by the corresponding velocity value [e.g., *Ganju and Schoellhamer*, 2006]. The correlation between cross-sectionally averaged turbidity and the velocity-weighted turbidity was above 0.96 at both sites (with regression slopes close to unity). Therefore, we neglected spatial correlations in the flux calculations.

3.4. Longitudinal Profiling

[17] Preliminary time series measurements of turbidity during March 2011 indicated the presence of an estuarine turbidity maximum (ETM) in the Transquaking River. Increases in turbidity at site FB1 occurred during the middle of flood tide and beginning of ebb tide while increases at site FB3 occurred only at the end of flood tide. This time series pattern is consistent with the oscillating mass concept presented by *Ganju et al*. [2004] and observed in several larger estuaries [*Grabemann and Krause*, 1994; *Grabemann et al*., 1997; *Uncles and Stephens*, 1993]. We profiled salinity and turbidity throughout a flood tide in the Transquaking River to confirm the presence of an ETM; a longitudinal transect spanning from Fishing Bay to approximately 8 km landward was traversed over a 6 h period (from slack-flood-slack).

3.5. Meteorological Data

[18] Hourly measurements of wind speed, wind direction, barometric pressure, and other atmospheric variables were retrieved from station CAMM2 (http://www.ndbc.noaa.gov/) located on the south shore of the Choptank River near Cambridge, Maryland. The station is 16 km north of the open-water region of Blackwater NWR and 23 km north of the confluence of the Transquaking River and Fishing Bay. Wind data were binned into speed and directional bins over the sediment flux measurement period to evaluate the influence of meteorological forcing on sediment flux.

[19] Winds at site CAMM2 were strongest (>10 m/s) from the northwest direction, coinciding with low-pressure systems and cold fronts moving west-to-east across the mid-Atlantic region. The most frequent winds were weak events (<5 m/s) from the south likely caused by land-ocean gradients in temperature (i.e., sea breeze). This pattern over the limited measurement period is similar to annual timescale wind forcing with changes in the relative frequency of storm events from the northwest. Wave data from the open water area of Blackwater NWR indicate that short-period waves (~1 s) with wave heights exceeding 0.30 m are common during the fall due to northwest winds (W. Boicourt, unpublished data, 2007).

4. Results

4.1. Continuous Tidal Water Fluxes

[20] ADCPs deployed in the tidal channels collected continuous time series of velocity at sites BWR and FB1. At site

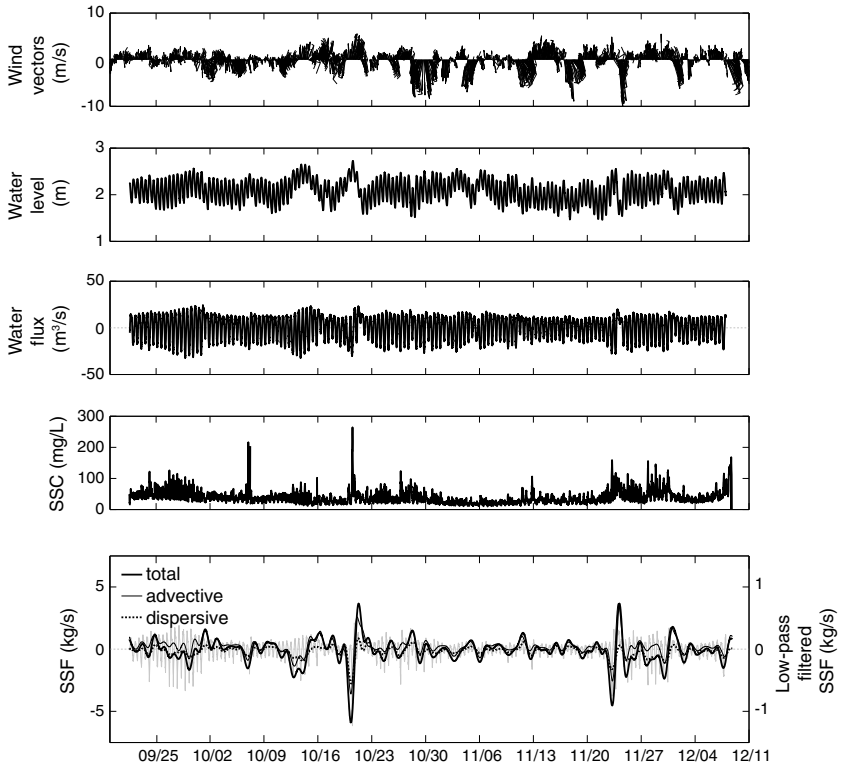

Figure 4. Time series of wind speed/direction, water level, tidal water flux, suspended sediment concentration (SSC), and suspended sediment flux (SSF) components at site FB1. Gray trace of SSF is tidal SSF; other terms are low-pass filtered. Positive water and sediment flux values indicate seaward transport. Wind vectors point in the direction the wind is going.

BWR, peak velocities reached 1.1 m/s on ebb and 1.0 m/s on flood, with a pronounced subtidal variability caused by barometric pressure fluctuations and/or wind forcing. At site FB1, peak velocities reached 0.90 m/s on ebb and 0.70 m/s on flood with larger spring-neap variability than site BWR, but substantial subtidal variability as well. Peak tidal water fluxes at site BWR were nearly 150 m^3/s on flood tide and 130 m^3/s on ebb tide; peak tidal water fluxes at site FB1 were 32 m^3/s on flood and 25 m^3/s on ebb (Figures 3 and 4).

4.2. Continuous Cross-Sectionally Averaged SSC

[21] SSC time series from site BWR show strong tidal variability with highest SSC (>400 mg/L) on ebb tides (Figure 2d); the highest SSC occur during a series of events corresponding with northerly winds (Figure 3). This is consistent with wind-wave generation over the open-water areas of Blackwater NWR causing resuspension and bank erosion (Figure 5). At site FB1, there is stronger spring-neap variability with episodic increases (SSC > 250 mg/L) during periods with strong southerly winds, corresponding to resuspension in Fishing Bay (Figure 4). Mean SSC were approximately 20% lower than data from spring 2011 [*Ganju et al*., 2012], though spectra behaved similarly.

4.3. Sediment Flux Decomposition

[22] At site BWR, net sediment flux was 1020 g/s in the seaward direction (Table 1). Net advective flux was the largest component (Figures 3 and 6), with a seaward direction that corresponded to northerly wind events that increased tidally averaged SSC and induced a seaward directed tidally averaged water flux (Figure 7) [*Salas-Monreal and Valle-Levinson*, 2008]. Net dispersive flux was roughly 30% of the total flux and also seaward. Dispersive flux followed advective flux, indicating that the same wind events that caused advective export also led to a tidal timescale correlation between ebb tide and increased SSC. Net Stokes drift was directed landward, but minor due

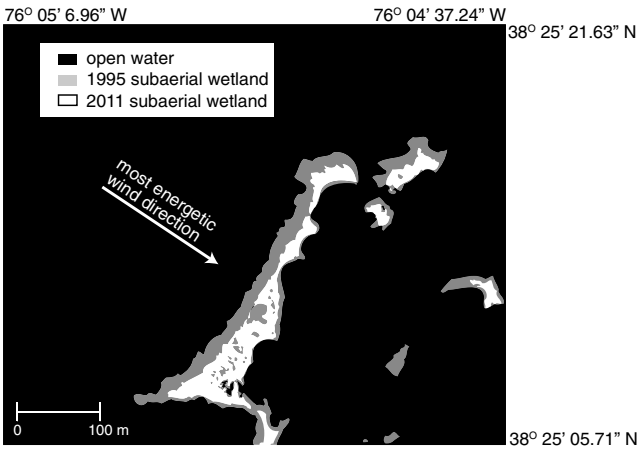

Figure 5. Change in subaerial wetland configuration from 1995 to 2011 over a selected portion of the Blackwater River wetland complex. Google Earth aerial imagery was converted to traced images using image software. Shoreline retreat corresponds to the most energetic wind (and ostensibly wave) direction as measured at Cambridge, MD.

Table 1. Net Flux Components Measured From Sites BWR and FB1 Over a 57 and 77 Day Period, Respectively[a]

	Site	
Sediment flux component	BWR	FB1
Advective ($<u><a><c>$)	820 g/s	42 g/s
Dispersive ($u'<a>c'$)	310 g/s	−34 g/s
Stokes drift ($u'a'<c>$)	−88 g/s	−32 g/s
Triple correlation ($u'a'c'$)	−11 g/s	−5 g/s
Total flux[b]	1020 ± 390 g/s	−31 ± 31 g/s
Total flux normalized by channel area	5.9 g/m^2/s	−0.7 g/m^2/s

[a]Positive values indicate export from the tidal channel.
[b]Random error and bias are combined and presented for total flux estimate but may apply to any of the flux components.

to the small changes in water level and channel cross-sectional area.

[23] At site FB1, net sediment flux was 31 g/s in the landward direction. At this site, net advective, dispersive, and Stokes drift fluxes were of relatively equal magnitude. Net advective flux was again directed seaward due to subtidal water export during periods with northerly winds (Figures 7 and 8). Net dispersive flux was landward due to a correlation between flood tide and increased SSC caused by a combination of a nearby seaward source of sediment (Fishing Bay and ultimately Chesapeake Bay) and a turbidity maximum located within the Transquaking River (see section below). Stokes drift flux was also directed landward and significant due to the phasing of flood tide and the high water mark. This phasing, characteristic of a progressive tidal wave, is possible due to a connection between the channel and significant open-water area landward of the measurement site. The typically minor triple correlation between Stokes drift and concentration was significant at this site, which highlights the advection of sediment during flood tide due to the ETM in the Transquaking River. This pattern can be seen in the slightly elevated SSC values at midflood tide (relative to ebb tide) at site FB1 (Figure 2d).

[24] *Ganju et al.* [2005] provided a comprehensive assessment of errors in tidal sediment flux estimation for wetland channels. Errors arise from the velocity measurements and calibrations, laboratory measurement of SSC, and cross-sectional variability. Following *Ganju et al.*'s [2005] methodology and substituting values appropriate for this study, we estimate a random error of 23% for both sites (230 g/s and 7.1 g/s for BWR and FB1, respectively), which is improved slightly from their estimate of 27%. The improvement arises from a more constrained SSC calibration in this study, due to a larger sample size. The largest potential bias in the flux measurement arises from small biases in the velocity measurement which can significantly change the direction of the advective flux [*Ganju and Schoellhamer*, 2006]. Biases in velocity do not affect dispersive or Stokes drift flux because the tidally averaged trend in velocity is removed to compute those terms. Biasing the velocity at site BWR by ±0.015 m/s (the error of the index velocity relationship; Figure 2a) modifies the total flux by ±160 g/s or ±16%. Flux estimates are more sensitive at site FB1 due to the small net flux; applying a ±0.015 m/s bias (Figure 2) creates a ±24 g/s (±77%) change in total flux though the direction of net sediment flux remains landward. Combining the potential random error and bias yields flux estimates of 1020 ± 390 g/s (BWR) and 31 ± 31 g/s (FB1).

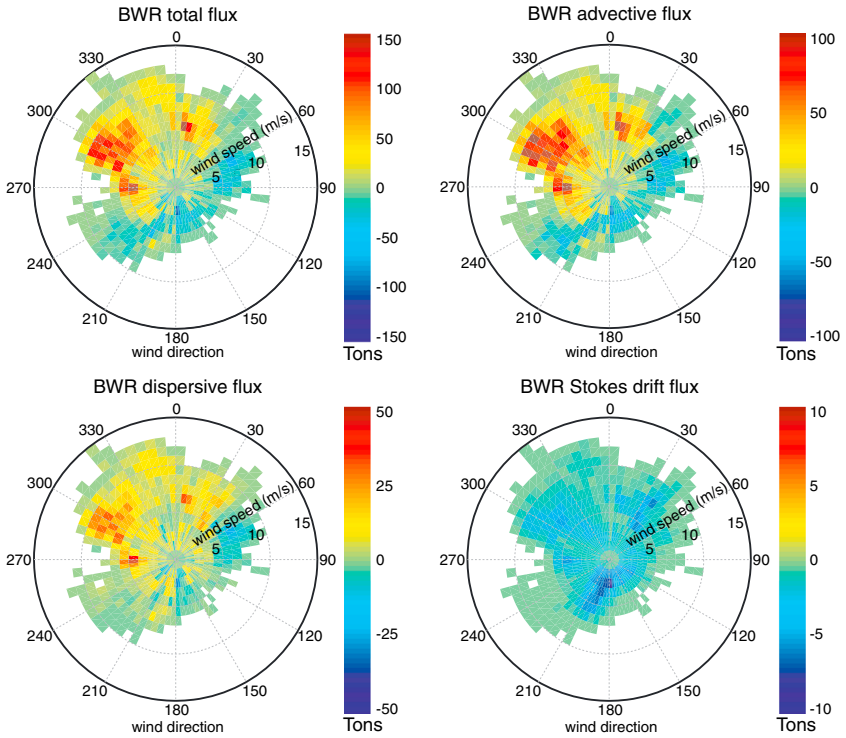

Figure 6. Cumulative sediment fluxes at site BWR, by component, as a function of wind direction (radial position) and speed (outward position), over the 20 September to 21 November 2011 period. Wind direction indicates direction the wind is coming from.

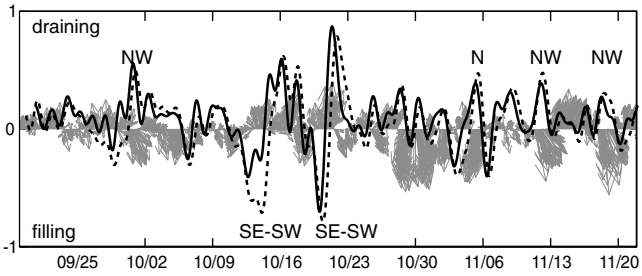

Figure 7. Normalized tidally averaged advective water flux in the two tidal channels (site BWR, dashed; site FB1, solid) and wind vectors. Winds from the north, northwest, and southwest tend to drain Chesapeake Bay, while winds from the southeast tend to fill [*Salas-Monreal and Valle-Levinson*, 2008].

4.4. Longitudinal Profiling

[25] Five transects at 10 stations on the Transquaking River were completed between 11:12 and 16:23 UTC on 6 October 2011, from slack-after-ebb to nearly the end of flood. The presence of a local turbidity maximum was confirmed; it is coincident with the advection of a salinity front from Fishing Bay near the time of maximum flood (Figure 9). A second ETM also appears at the limit of salinity intrusion at midflood tide. The primary ETM during this period was centered approximately 1 km landward of the entrance to the FB1 tidal creek. Tidal forcing during the survey appeared substantially weaker than the prior spring tide when SSC at site FB1 (Figure 4) peaked at approximately 100 mg/L; during this survey, maximum SSC at site FB1 was 50 mg/L. Changes in tidal forcing due to the spring-neap cycle likely alter both the longitudinal and vertical distribution of the ETM [*Talke et al.*, 2009].

5. Discussion

5.1. Atmospheric and Tidal Controls on Sediment Transport

[26] The relative magnitude of the sediment flux components at the sites BWR and FB1 illustrates the extent to which atmospheric forcing, mainly winds and barometric pressure fluctuations, can dominate sediment fluxes to tidal wetlands. Site BWR drains a large open-water expanse that is vulnerable to wind-wave action during almost any wind direction, but especially the dominant northwest winds. This wind-wave action may resuspend unconsolidated, organic-rich sediments on the submerged marsh plain, erode intertidal mudflats at the base of marsh bluffs, and directly erode marsh bluffs (Figure 5). In a closed, lacustrine system, this would not cause a net sediment loss but Chesapeake Bay as a whole responds barotropically to wind forcing with draining of the bay during northerly, northwesterly, and southwesterly winds; the bay fills under southeasterly, northeasterly, and easterly winds [*Salas-Monreal and Valle-Levinson*, 2008]. The two peripheral tidal channels in this study appear to respond to this larger-scale forcing similarly: Northerly, northwesterly, and southwesterly winds export water from the channels on the subtidal timescale, while southeasterly winds import water (Figure 7). This subtidal water (and sediment) export is manifested in the large seaward advective flux term

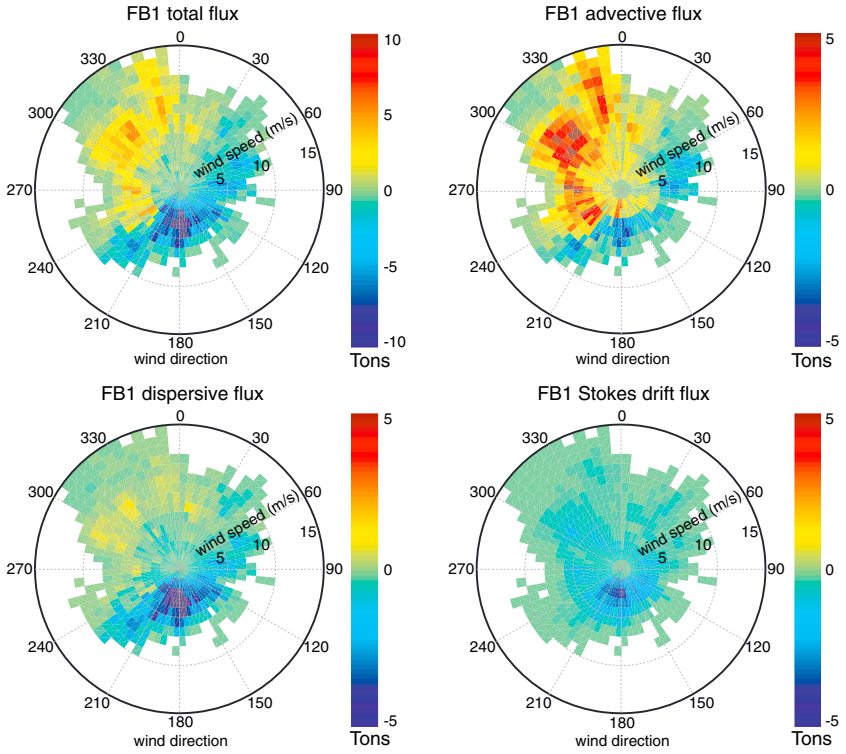

Figure 8. Cumulative sediment fluxes at site FB1, by component, as a function of wind direction (radial position) and speed (outward position), over the 20 September to 7 December 2011 period. Wind direction indicates direction the wind is coming from.

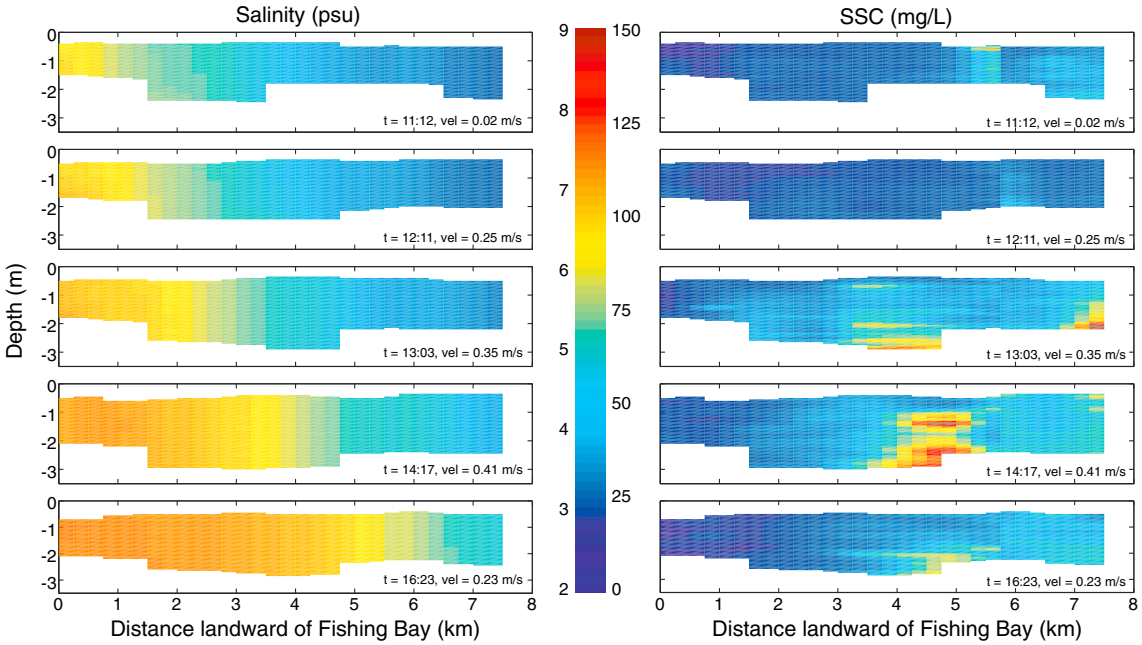

Figure 9. Longitudinal transects of salinity and SSC in the Transquaking River channel, on 6 October 2011. Times are in UTC. Velocities correspond to site FB1, off the Transquaking River and are flood directed. Labels to the left of the color bar correspond to salinity; labels to the right correspond to SSC. The entrance to the FB1 tidal channel is approximately at 3.5 km.

which dominates transport at site BWR. Though the dispersive flux mechanism also tends to export sediment (due to a spatial gradient in SSC from landward to seaward), the combined tidal components of the sediment flux account for less than a third of the total transport. The only mechanisms that can reliably transport sediment landward past site BWR are tidal forces during periods of southerly winds (Figure 6). Tidal timescale processes alone (represented by dispersive and Stokes drift flux components) during periods of quiescent winds are responsible for less than 11% of the net transport through the cross section. Half of the net sediment flux occurs during 3 days (out of a total of 80 days) coinciding with the passage of cold fronts or northeast moving low-pressure systems (Figure 3; 21 and 28 October and 11 November 2011).

[27] Conversely, site FB1 demonstrates a more nuanced balance between wind and tidal forces (Figure 8). The advective water and sediment flux response to northwest winds is virtually identical to site BWR and demonstrates the influence of Chesapeake Bay circulation on exchange in peripheral tidal channels as well as wetland sediment supply (Figure 7). However, the proximity to Fishing Bay allows tidal forcing (dispersive, Stokes drift, and triple correlation term) to counteract the subtidal advective flux during periods of weaker winds. Net dispersive flux is landward due to higher SSC in the Transquaking River ETM as opposed to the terminal end of the tidal channel, which leads to sediment import on flood tides. Stokes drift flux, which quantifies the flux due to correlation between flood tide velocity and high water, is relatively large due to the nearly progressive nature of the tidal wave (i.e., maximum flood occurs close to high tide). While some of the ETM signal is manifested in the dispersive and Stokes drift flux components, the triple correlation between velocity, high tide, and concentration is a clear signature of the ETM's influence as it advects into the channel on flood tide. This correlation is manifested as elevated SSC during periods of high flood tide velocity (relative to ebb tide; Figure 2d), as a mobile sediment mass is resuspended from the bed of the Transquaking River; this increase in SSC during peak velocity and high tide leads to a large landward flux. This flux is maximized during spring tides when tidal forcing is greatest; during the 25 September to 2 October 2011 time period, this term accounts for 25% of the net sediment flux. Tidal timescale net transport (landward) during quiescent winds is more than 80% of the net advective flux during the entire measurement period (in the opposing direction). However, two large weather events (Figure 4; 21 October and 23 November 2011) import 25% of the net flux over a total of 5 days. It should be noted that considering the error, the net flux may be close to 0. Nonetheless, the mechanisms leading to sediment import versus export are useful for evaluating the system's response to changes in forcing.

5.2. Scaling Sediment Transport Relative to Sea Level Rise and Marsh Loss

[28] The net sediment import to the Transquaking complex (31 g/s), distributed over the marsh plain, approaches the local rate of relative sea level rise (3.50 mm/yr; http://www.tidesandcurrents.noaa.gov/sltrends/sltrends.shtml). Applying a channel drainage area of 1.4 km^2 (based on aerial photography) and a measured dry bulk density of 180 kg/m^3 yields a vertical accretion rate of 3.9 mm/yr. Measured accretion rates at nearby sites range between 3 and 5 mm/yr (G. R. Guntenspergen, unpublished data, 2013). While the majority of sediment advected into the channel on the tidal timescale does not directly deposit on the marsh plain, the net sediment budget indicates that this rate of sediment import, barring shallow subsidence, is sufficient to maintain supply relative

Table 2. Conceptual Model of Channel Sediment Flux Portfolio as Applied to Four Wetlands From Chesapeake (Blackwater, Transquaking) and San Francisco Bays (Browns Island, Petaluma)

	Blackwater	Transquaking	Browns Island	Petaluma
Source				
River			X	X
Marine		X	X	X
Internal (ETM)		X		X
Wetland	X			
Location				
River-adjacent			X	X
Landward			X	
Seaward		X		X
Self-adjacent	X			
Mobilization				
River runoff			X	X
Tides		X		X
Wind-waves	X	X	X	X
Advection				
River			X	X
Tides		X	X	X
Subtidal	X	X	X	

to sea level rise over the longer term. Processes such as compaction, root zone collapse, and longer-term changes in supply from Fishing Bay (via Chesapeake Bay) [*Cheng et al*., 2013] may alter the import and stability trajectory however. Given the associated error, the accretion may actually range from near 0 to 8 mm/yr. It should also be noted that we are not delineating between inorganic and organic accretion for this estimate. Suspended sediment samples averaged 30% organic content based on loss-on-ignition (N. K. Ganju, unpublished data, 2013) so we are assuming similar organic content of any deposited mass.

[29] At the Blackwater River complex, the sediment budget of the complex landward of site BWR is influenced by local sources (erosion) and sinks (deposition on the marsh platform) of sediment. Sediment deposition rates on Blackwater River marshes average about 6.0 mm/yr (G. R. Guntenspergen, unpublished data, 2013). Extrapolating this deposition rate across the entire subaerial marsh plain (30 km^2) using a locally derived dry bulk density (160 kg/m^3) yields a total sediment deposition rate of 900 g/s. While this is likely an overestimate (sediment deposition rates were measured close to river edges and would be expected to be less in interior locations), it implies that a significant amount of sediment eroded from subaqueous sources is trapped on the marsh rather than being exported through the Blackwater River. Since external sources of sediment are small, the total amount of sediment removed from the subaqueous plain is the sediment flux measured at BWR (1020 g/s) plus the sediment flux trapped on the marsh surface (900 g/s), or approximately 1900 g/s.

[30] Vertical erosion of the large open-water bay is the dominant source of the ~1900 g/s sediment flux passing through the Blackwater River complex. Loss of intertidal wetlands in the system occurs at a current rate of 0.4 km^2/yr [*Stevenson et al*., 1985]. If we assume that vertical erosion takes place in the entire upper 0.12 m (roughly the elevation range of intertidal vegetation at Blackwater NWR) [*Kirwan and Guntenspergen*, 2012], the sediment flux attributable to this source is 240 g/s. Vertical erosion of the large open-water bay and subaqueous erosion of marsh edges and interior ponds must explain the remainder of the sediment flux (~1700 g/s). Averaged over the entire open-water bay (32 km^2), the remaining sediment flux implies an erosion rate of 0.011 m/yr. Thus, vertical erosion of the large open-water bay rather than loss of intertidal wetlands is likely the source of the majority of sediment exported out of the Blackwater River complex.

[31] Extrapolating these seasonal measurements may introduce error on the annual-to-decadal timescale. However, wind forcing during this period is overall similar to the annual pattern in terms of speed and direction, suggesting that the seasonal net sediment export at site BWR is a reasonable extrapolation on the annual timescale. At site FB1, tidal forcing is expectedly consistent and would result in similar fluxes on annual timescales. Ideally, measurements would span an entire year to capture seasonal variability, especially in systems with seasonal sediment supply from river flows. The flux decomposition approach proves useful in separating the forcing mechanisms, thereby delineating the seasonal components of the fluxes.

5.3. Sediment Fluxes as a Wetland Stability Indicator: Illustrating a Conceptual Model

[32] The dramatic differences in sediment transport and stability between these two sites and sites from other studies allow us to draw general inferences about the role of channel sediment fluxes on marsh stability. A conceptual model for the role of sediment fluxes should account for (1) the location of the dominant sediment source, (2) the location of the wetland relative to the source, (3) the mobilization mechanism and timescale of the sediment source, and (4) the advection mechanism and timescale of the mobilized sediment. *Friedrichs and Perry* [2001] and many other studies have covered these topics, but here we specifically discuss them in the context of sediment transport to the tidal channel and the resulting stability.

[33] With the conceptual model, one can identify the potential stability of wetland complexes by assembling a portfolio of sediment transport characteristics. In an idealized context, a stable complex would receive sediment from consistent external sources, and mobilization and advection would take place with regularity. The distance between the external source and wetland should also be less than a tidal excursion (defined as a mean tidal velocity multiplied by the time of a single tidal phase, e.g., 6.21 h). Tidal excursion characterizes a tidal transport length and is a good proxy for connectivity: Wetland channels within one tidal excursion of the source will benefit from a steady supply on the tidal timescale. For realistic examples, the two complexes from this study and two complexes from San Francisco Bay are used to illustrate the conceptual model and indicate potential stability. These four wetlands span the full range of sediment sources and transport mechanisms. When the features are considered as a sediment transport portfolio, it becomes evident that wetlands with a reliable portfolio may be inherently more stable under future scenarios of change (Table 2 and Figure 10).

5.3.1. Blackwater River Complex

[34] The Blackwater River complex is characterized by the following features: an internal sediment source from wetland collapse and shoreline retreat [*Stevenson et al*., 1985], no distance between the source and wetland complex, mobilization

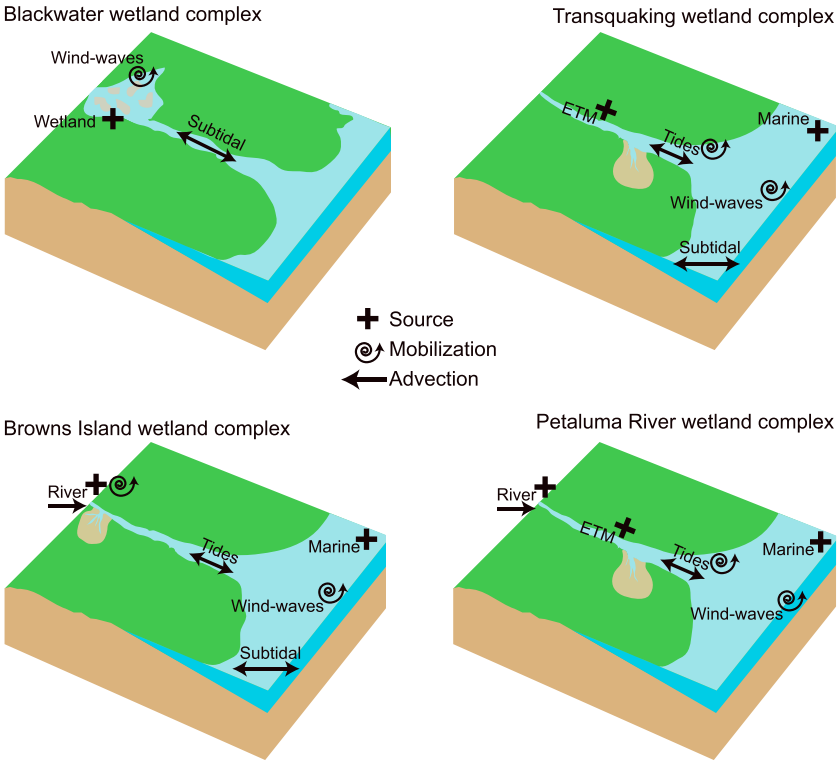

Figure 10. Illustrations of conceptual model for four wetland complexes. All but the Blackwater complex have a diverse portfolio of external sediment sources, mobilization mechanisms, and advection mechanisms.

from wind-wave resuspension, and advection from subtidal forcing. The internal sediment source manifests as appreciable SSC (Table 3) generated by waves over the open-water area and impacting marsh shorelines. Despite a significant tidal velocity in the main drainage channel, velocities and tidal range within the system are small; a high estimate of the tidal excursion is 8 km (based on a mean tidal velocity in the channel). This prevents transport from the nearest external source, Fishing Bay, which is 25 km from the majority of the system. While the channel may import sediment over several tidal cycles, a single wind event may force enough water out to export sediment from the channel and back to Fishing Bay. The remaining marsh plain adjacent to the open-water areas is accreting sediment but lateral retreat will eventually erode the marsh plain despite the vertical movement [*Mariotti and Fagherazzi*, 2013]. The vast open-water areas with a fetch approaching 10 km create an environment conducive to sediment mobilization during windy periods (especially from the northwest); the subtidal advection caused by these same winds lead to sediment export. This complex will continue to be unstable mainly due to the lack of an external sediment source from either the landward or seaward ends. Given the conceptual model, it would appear that this complex originally had a significant watershed sediment supply from land clearing [*Brush*, 2001] or more hydraulic connectivity with Chesapeake Bay from the northwestern end of the complex. Subsequent reductions in load or tidal connectivity may have spurred the degradation of the complex (in addition to herbivory and sea level rise). The well-documented conversion of wetland plain to open-

Table 3. Characteristic Sediment Transport Values for Four Wetland Systems

	Tide Range (m)	Tidal Velocity (m/s)	Tidal Excursion (km)	Distance to Nearest External Sediment Source (km)	SSC (mg/L)	Peak Wave Height (m)	Peak River Flow (m^3/s)
Blackwater	0.20	0.60	8.0	25	55	0.30	14[a]
Transquaking	0.60	0.50	5.0	3.5	40	0.40[b]	27[a]
Browns Island	1.0[c]	0.30[c]	3.4[c]	2.0	20[c]	0.60[d]	17,000[e]
Petaluma River	2.0[f]	0.50[f]	5.6[f]	<1.0	500[f]	0.60[g]	120[a]

[a]http://waterdata.usgs.gov.
[b]*U.S. Army Coastal Engineering Research Center* [1984].
[c]*Ganju et al.* [2005].
[d]*Jones and Monismith* [2008].
[e]http://www.water.ca.gov/dayflow/.
[f]*Ganju et al.* [2004].
[g]*Schoellhamer et al.* [2008]; all other values are from this study.

water area is the clearest indicator of instability, but the sediment flux characteristics also suggest that sediment import over any significant timescale is unlikely.

5.3.2. Transquaking River Complex

[35] The wetland complex adjacent to the Transquaking River offers a stark contrast to the Blackwater complex: There is an external sediment source from Fishing Bay and a local ETM; the wetland resides within a tidal excursion (5 km) of both sources, which are no more than 3.5 km away; mobilization occurs from both tidal resuspension of a mobile sediment mass and from wind-wave resuspension in Fishing Bay; and transport is due to both tidal and subtidal advection over varying timescales (Table 3). Wind-waves in Fishing Bay approach 0.4 m, which can induce a significant stress on the sediment bed given depths of less than 3 m. Chesapeake Bay and its watershed may be responsible for replenishment of sediment in Fishing Bay on a seasonal timescale [*Cheng et al*., 2013]. Wind-wave resuspension combined with tidal advection can replenish the ETM while also directly advecting sediment into the wetland channel. The diversity of source locations, mobilization mechanisms, and advection mechanisms illustrates the sustainability of sediment fluxes to this complex. Ultimately the proximity and reliability of the sediment source result in a prognosis of stability over the near term. However, reductions of the sediment load to Chesapeake Bay could affect this system's stability over the decadal timescale.

5.3.3. Browns Island, San Francisco Bay

[36] Browns Island, a wetland complex located at the landward end of San Francisco Bay (Suisun Bay) near the confluence of the Sacramento and San Joaquin Rivers, has persisted over a few millennia [*Goman and Wells*, 2000]. *Ganju et al*. [2005] measured sediment fluxes in the main tidal channel of Browns Island. That study pointed to the dominant role of an external seaward sediment source and mobilization mechanism (wind-wave resuspension), tidal advection, and subtidal advection from changes in water level gradient. While tidal excursion is comparatively small (Table 3), the nearest sediment source is at the terminus of the short tidal channel: the Sacramento-San Joaquin River Delta. *Reed* [2002] highlighted increased sediment delivery to the marsh plain during river flow events from the delta. Wind-waves over Grizzly Bay, a nearby sediment-rich subembayment of Suisun Bay, are large enough to also provide a reliable external sediment source. However, Suisun Bay and San Francisco Bay as a whole have undergone a transition from being sediment convergent and depositional to sediment divergent and erosional over the nineteenth and twentieth centuries [*Gilbert*, 1917; *Cappiella et al*., 1999]. This change is largely due to a reduction in watershed sediment delivery [*Wright and Schoellhamer*, 2004] since the peak delivery during hydraulic mining of the Sierra Nevada. Reduced loads will likely threaten the long-term reliability of the sediment portfolio, but continued redistribution of in-bay sediments may provide a short-term sediment source during the prolonged wind-wave season.

5.3.4. Petaluma River Marsh, San Francisco Bay

[37] *Siegel* [2002] investigated the morphological evolution of a restored tidal marsh in San Francisco Bay, near the junction of the tidal Petaluma River and San Pablo Bay subembayment. This complex was a subsided diked plain that was opened to tidal action in 1994. Subsequently, the marsh accreted rapidly and developed into a well-colonized wetland complex. *Ganju et al*. [2004] later identified a persistent ETM and oscillating sediment mass located within the Petaluma River channel, directly adjacent to the restored marsh. Suspended sediment concentrations in the channel exceeded 4000 mg/L on spring tides and provided a nearby source of sediment on flood tides; the large tidal excursion (Table 3) allows sediment from the Petaluma River and San Pablo Bay to reach the wetland complex. Mobilization was due to tidal resuspension on both flood and ebb tides; sediment that enters the complex on flood is trapped by a reduction in velocity and unable to leave on ebb tide. The oscillating sediment mass and ETM were replenished by both seasonal river delivery (with a characteristic river SSC of 500 mg/L) and erosion of seaward mudflats during the wind-wave season. Waves over the large expanse of San Pablo Bay can exceed 0.6 m and erode the fringing mudflats which are widespread in the area. From a stability standpoint, this complex has a reliable portfolio that consists of a river source, tidal advection, and a persistent ETM with high concentrations of suspended sediment.

5.4. Reliable Sediment Portfolios and Inferring Future Wetland Stability

[38] The case studies presented above describe a range of wetland locations, sediment sources, and mobilization mechanisms. Evaluating these characteristics yields a qualitative understanding of each wetland complex's potential for future stability. For example, there appears to be no reliable future mechanism to supply the Blackwater complex with suspended sediment, barring reconnection with a watershed sediment source or increased tidal advection. Conversely, both the Transquaking and Petaluma Rivers complexes appear to have a reliable sediment supply from seaward sources that are not yet depleted (Fishing and San Pablo Bays, respectively). The conceptual model presented here can be applied to any wetland complex, and the individual elements of the sediment portfolio can be evaluated for reliability. This yields a qualitative metric for inferring wetland stability with a general understanding of the hydrodynamic and sediment transport mechanisms.

[39] From a resource management point-of-view, seaward wetlands in some areas may be more viable over the next few decades than landward wetlands with decreased tidal influence and negligible watershed sediment supply. Eventually, seaward wetlands may be cut off from the mainland (and ultimately submerged) but in the short term they may serve as important buffers for wildlife and coastal protection. This process is counterintuitive to the traditional marine transgression concept, where there is a steady landward movement of landforms under sea level rise, but is certainly evident in the two Chesapeake Bay complexes studied here.

6. Conclusion

[40] Sediment flux measurements through tidal wetland channels are an integrative metric that gauges both the sediment budget of the wetland complex and the mechanisms controlling transport. Complexes that export sediment during typical forcing conditions are unlikely to be stable due to ongoing sea level rise. Two adjacent wetland complexes

peripheral to Chesapeake Bay demonstrate the influence of atmospheric and tidal processes on sediment transport to the wetland complex. Both complexes respond to regional circulation: tidal channels drain and fill on the subtidal timescale in step with Chesapeake Bay, thereby linking the peripheral areas with the larger basin. The Blackwater River complex, unstable over the past several decades, exported sediment at a rate of 0.56 $kg/m^2/yr$ largely due to wind-wave resuspension over open-water areas and subsequent advection through this regional circulation processes. Conversely, the currently stable Transquaking River complex imported 0.70 $kg/m^2/yr$ due to strong tidal forcing that provides sediment from marine and ETM sources. The level of import matches the current rate of relative sea level rise and is a positive contribution to marsh vertical elevation. These results suggest that seasonal timescale sediment flux measurements are good indicators of longer-term marsh stability. A conceptual model based on these two systems and two others in San Francisco Bay suggests that wetlands with a reliable portfolio of sediment sources and transport mechanisms may be more stable over the near term. Though counterintuitive, it appears that in some cases, seaward wetlands may be temporarily more resilient to sea level rise than landward wetlands with no access to an external sediment source.

[41] **Acknowledgments.** This study would not have been possible without the considerable assistance of Jonathan Borden, Patrick Brennand, Patrick Dickhudt, Kyle Derby, Sandy Baldwin, Ellyn Montgomery, Marinna Martini, Maitane Olabarrieta, and Christine Sabens. William Boicourt generously provided wave data. Funding was provided by the USGS Coastal and Marine Geology Program and the Climate and Land Use Change Research and Development Program. Constructive comments were provided by Giulio Mariotti, Andrew Ashton, Alexander Densmore, David Schoellhamer, Don Cahoon, Glenn Guntenspergen, Richard Signell, and two anonymous reviewers. Background for the conceptual model diagram was courtesy of the Integration and Application Network, University of Maryland Center for Environmental Science (ian.umces.edu/symbols/). Use of brand names is for identification purposes only and does not constitute endorsement by the U.S. Government.

References

Bertness, M. D. (1984), Ribbed mussels and Spartina Alterniflora production in a New England salt marsh, *Ecology*, *65*, 1794–1807, doi:10.2307/1937776.

Brush, G. S. (2001), Natural and anthropogenic changes in Chesapeake Bay during the last 1000 years, *Hum. Ecol. Risk Assess.*, *7*, 1283–1296, doi:10.1080/20018091095005.

Cahoon, D. R., and R. E. Turner (1989), Accretion and canal impacts in a rapidly subsiding wetland II. Feldspar marker horizon technique, *Estuaries Coasts*, *12*, 260–268.

Cahoon, D. R., J. W. Day Jr., and D. J. Reed (1999), The influence of surface and shallow subsurface soil processes on wetland elevation: A synthesis, *Curr. Topics Wetland Biogeochem.*, *3*, 72–88.

Cappiella, K., C. Malzone, R. Smith, and B. Jaffe (1999), Sedimentation and bathymetry changes in Suisun Bay, 1867–1990, *U.S. Geological Survey Open File Report*, 99–563.

Cheng, P., M. Li, and Y. Li (2013), Generation of an estuarine sediment plume by a tropical storm, *J. Geophys. Res. Oceans*, *118*, 856–868, doi:10.1002/jgrc.20070.

D'Alpaos, A., S. Lanzoni, M. Marani, and A. Rinaldo (2007), Landscape evolution in tidal embayments: modeling the interplay of erosion sedimentation and vegetation dynamics, *J. Geophys. Res.*, *112*, F01008, doi:10.1029/2006JF000537.

D'Alpaos, A., C. Da Lio, and M. Marani (2012), Biogeomorphology of tidal landforms: Physical and biological processes shaping the tidal landscape, *Ecohydrology*, *5*, 550–562, doi:10.1002/eco.279.

Day, J. W., G. P. Kemp, D. J. Reed, D. R. Cahoon, R. M. Boumans, J. M. Suhayda, and R. Gambrell (2011), Vegetation death and rapid loss of surface elevation in two contrasting Mississippi delta salt marshes: The role of sedimentation, autocompaction and sea-level rise, *Ecol. Eng.*, *37*, 229–240, doi:10.1016/j.ecoleng.2010.11.021.

Deegan, L. A., D. S. Johnson, R. S. Warren, B. J. Peterson, J. W. Fleeger, S. Fagherazzi, and W. M. Wollheim (2012), Coastal eutrophication as a driver of salt marsh loss, *Nature*, *490*, 388–392, doi:10.1038/nature11533.

DeLaune, R. D., and S. R. Pezeshki (1994), The influence of subsidence and saltwater intrusion on coastal marsh stability: Louisiana Gulf Coast, U.S. A., *J. Coastal Res.*, Special Issue *12*, 77–89.

Fagherazzi, S., L. Carniello, L. D'Alpaos, and A. Defina (2006), Critical bifurcation of shallow microtidal landforms in tidal flats and salt marshes, *Proc. Natl. Acad. Sci. U. S. A.*, *103*, 8337–8341, doi:10.1146/annurev.earth.35.031306.140128.

Fagherazzi, S., et al. (2012), Numerical models of salt marsh evolution: Ecological, geomorphic, and climatic factors, *Rev. Geophys.*, *50*, RG1002, doi:10.1029/2011RG000359.

Ford, M. A., and J. B. Grace (1998), Effects of vertebrate herbivores on soil processes, plant biomass, litter accumulation and soil elevation changes in a coastal marsh, *J. Ecology*, *86*, 974–982, doi:10.1046/j.1365-2745.1998.00314.x.

Friedrichs, C. T., and J. E. Perry (2001), Tidal salt marsh morphodynamics: A synthesis, *J. Coastal Res*, Special Issue *27*, 7–37.

Gabet, E. (1998), Lateral migration and bank erosion in a salt marsh tidal channel in San Francisco Bay, California, *Estuaries*, *21*, 745–753.

Ganju, N. K., and D. H. Schoellhamer (2006), Annual sediment flux estimates in a tidal strait using surrogate measurements, *Estuarine Coastal Shelf Sci.*, *69*, 165–178, doi:10.1016/j.ecss.2006.04.008.

Ganju, N. K., D. H. Schoellhamer, J. C. Warner, M. F. Barad, and S. G. Schladow (2004), Tidal oscillation of sediment between a river and a bay a conceptual model, *Estuarine Coastal Shelf Sci.*, *60*, 81–90, doi:10.1016/j.ecss.2003.11.020.

Ganju, N. K., D. H. Schoellhamer, and B. A. Bergamaschi (2005), Suspended sediment fluxes in a tidal wetland: measurement, controlling factors, and error analysis, *Estuaries*, *28*, 812–822, doi:10.1007/BF02696011.

Ganju, N. K., P. J. Dickhudt, E. T. Montgomery, P. Brennard, R. K. Derby, T. W. Brooks, G. R. Guntenspergen, M. A. Martini, J. Borden, and S. M. Baldwin (2012), Summary of oceanographic and water-quality measurements near the Blackwater National Wildlife Refuge, Maryland, 2011: *U.S. Geological Survey Open-File Report* 2012–1099. [Available at http://pubs.usgs.gov/of/2012/1099/.]

Geyer, W. R., J. D. Woodruff, and P. Traykovski (2001), Sediment transport and trapping in the Hudson River estuary, *Estuaries Coasts*, *24*, 670–679.

Gilbert, G. K. (1917), Hydraulic-mining debris in the Sierra Nevada, (No. 105–107), United States Government Printing Office.

Goman, M., and L. Wells (2000), Trends in river flow affecting the northeastern reach of the San Francisco Bay estuary over the past 7000 years, *Quaternary Res.*, *54*, 206–217, doi:10.1006/qres.2000.2165.

Grabemann, I., and G. Krause (1994), Suspended matter fluxes in the turbidity maximum of the Weser estuary, in *Changes in Fluxes in Estuaries*, edited by K. R. Dyer and R. J. Orth, Olsen & Olsen, Denmark, pp. 23–28.

Grabemann, I., R. J. Uncles, G. Krause, and J. A. Stephens (1997), Behaviour of turbidity maxima in the Tamar (UK) and Weser (FRG) estuaries, *Estuarine Coastal Shelf Sci.*, *45*, 235–246.

Helsel, D. R., and R. M. Hirsch (1992), *Statistical methods in water resources*, 49 pp., Elsevier Science Publications, the Netherlands.

Hood, W. G. (2010), Tidal channel meander formation by depositional rather than erosional processes: examples from the prograding Skagit River Delta (Washington, USA), *Earth Surf. Process. Landforms*, *35*, 319–330.

Jones, N. L., and S. G. Monismith (2008), The influence of whitecapping waves on the vertical structure of turbulence in a shallow estuarine embayment, *J. Phys. Oceanogr.*, *38*, 1563–1580, doi:10.1175/2007JPO3766.1.

Kirwan, M. L., and G. R. Guntenspergen (2012), Feedbacks between inundation, root production, and shoot growth in a rapidly submerging brackish marsh, *J. Ecol.*, *100*, 764–770.

Kirwan, M. L., and A. B. Murray (2007), A coupled geomorphic and ecological model of tidal marsh evolution, *Proc. Nat. Acad. Sci. U.S.A.*, *104*, 6118–6122, doi:10.1073/pnas.0700958104.

Kirwan, M. L., A. B. Murray, and W. S. Boyd (2008), Temporary vegetation disturbance as an explanation for permanent loss of tidal wetlands, *Geophys. Res. Lett.*, *35*, L05403, doi:10.1029/2007GL032681.

Marani, M., A. D'Alpaos, S. Lanzoni, L. Carniello, and A. Rinaldo (2007), Biologically controlled multiple equilibria of tidal landforms and the fate of the Venice lagoon. *Geo. Res. Lett.*, *34*, L11402, doi:10.1029/2007GL030178s.

Mariotti, G., and S. Fagherazzi (2013), Critical width of tidal flats triggers marsh collapse in the absence of sea-level rise, *Proc. Natl. Acad. Sci. U. S. A.*, *110*, 5353–5356, doi:10.1073/pnas.1219600110.

Mueller, D. S., and C. R. Wagner (2009), Measuring discharge with acoustic Doppler current profilers from a moving boat, *U.S. Geological Survey Techniques and Methods*, 3A-22, 72.

Redfield, A. C. (1972), Development of a New England salt marsh, *Ecol. Monogr.*, *42*, 201–237, doi:10.2307/1942263.

Reed, D. J. (2002), Understanding tidal marsh sedimentation in the Sacramento-San Joaquin delta, California, *J. Coastal Res.*, Special Issue *36*, 605–611.

Reed, D. J., T. Spencer, A. L. Murray, J. R. French, and L. Leonard (1999), Marsh surface sediment deposition and the role of tidal creeks: Implications for created and managed coastal marshes, *J. Coastal Conservation*, *5*, 81–90, doi:10.1007/BF02802742.

Ruhl, C. A., and M. R. Simpson (2005), Computation of discharge using the index-velocity method in tidally affected areas, *U.S. Geological Survey Scientific Investigations Report* 2005–5004, http://pubs.usgs.gov/sir/2005/5004.

Salas-Monreal, D., and A. Valle-Levinson (2008), Sea-level slopes and volume fluxes produced by atmospheric forcing in estuaries: Chesapeake Bay case study, *J. Coastal Res.*, *24*, 208–217, doi:10.2112/06-0632.1.

Sallenger, A. H., Jr., K. S. Doran, and P. A. Howd (2012), Hotspot of accelerated sea-level rise on the Atlantic coast of North America, *Nat. Clim. Change*, doi:10.1038/nclimate1597.

Scheffer, M., S. Carpenter, J. A. Foley, C. Folkes, and B. Walker (2001), Catastrophic shifts in ecosystems, *Nature*, *413*, 591–596.

Schoellhamer, D. H., N. K. Ganju, and G. G. Shellenbarger (2008), Sediment transport in San Pablo Bay, in *Technical Studies for the Aquatic Transfer Facility: Hamilton Wetlands Restoration Project*, edited by D. A. Cacchione and P. A. Mull, pp. 36–107, U.S. Army Corps of Engineers, San Francisco District.

U.S. Army Coastal Engineering Research Center (1984), Shore protection manual, Department of the Army, Corps of Engineers, U.S. Govt. Printing Office, Washington, D. C., USA.

Siegel, S. W. (2002), Slough channel network and marsh plain morphodynamics in a rapidly accreting tidal marsh restoration on diked, subsided baylands: San Francisco Estuary, California. UC San Diego: California Sea Grant College Program. Retrieved from: http://escholarship.org/uc/item/9v93618k.

Stevenson, J. C., M. S. Kearney, and E. C. Pendleton (1985), Sedimentation and erosion in a Chesapeake Bay brackish marsh system, *Mar. Geol.*, *67*, 213–235, doi:10.1016/0025-3227(85)90093-3.

Talke, S. A., H. E. De Swart, and H. M. Schuttelaars (2009), Feedback between residual circulations and sediment distribution in highly turbid estuaries: An analytical model, *Cont. Shelf Res.*, *29*, 119–135, doi:10.1016/j.csr.2007.09.002.

Temmerman, S., T. J. Bouma, J. Van de Koppel, D. Van der Wal, M. B. De Vries, and P. M. J. Herman (2007), Vegetation causes channel erosion in a tidal landscape, *Geology*, *35*, 631–634.

Temmerman, S., P. Moonen, J. Schoelynck, G. Govers, and T. J. Bouma (2012), Impact of vegetation die-off on spatial flow patterns over a tidal marsh, *J. Geophys. Res. Lett.*, *39*, L03406, doi:10.1029/2011GL050502.

Uncles, R. J., and J. A. Stephens (1993), Nature of the turbidity maximum in the Tamar Estuary, U.K, *Estuarine Coastal Shelf Sci.*, *36*, 413–431, doi:10.1006/ecss.1993.1025.

van der Wal, D., and K. Pye (2004), Patterns, rates and possible causes of saltmarsh erosion in the Greater Thames area (UK), *Geomorphology*, *61*, 373–391.

Wang, D.-P., and A. J. Elliott (1978), Non-tidal variability in the Chesapeake Bay and Potomac River: Evidence for non-local forcing, *J. Phys. Oceanogr.*, *8*, 225–232.

Webb, E. L., D. A. Friess, K. W. Krauss, D. R. Cahoon, G. R. Guntenspergen, and J. Phelps (2013), A global standard for monitoring coastal wetland vulnerability to accelerated sea-level rise, *Nat. Clim. Change*, *3*, 458–465.

Wright, S. A., and D. H. Schoellhamer (2004), Trends in the sediment yield of the Sacramento River, California, 1957–2001, *San Francisco Estuary and Watershed Science*, *2*(2), 11–24.